arXiv:1211.4690v2 [cond-mat.mtrl-sci] 28 Nov 2012

Unfolding first-principles band structures with a non-orthogonal basis set: a study on surface and vacancy states of ZrB_2

Chi-Cheng Lee (李啓正),[1] Yukiko Yamada-Takamura,[1] and Taisuke Ozaki[1, 2]

[1]*School of Materials Science, Japan Advanced Institute of Science and Technology (JAIST), 1-1 Asahidai, Nomi, Ishikawa 923-1292, Japan*

[2]*Research Center for Simulation Science, Japan Advanced Institute of Science and Technology (JAIST), 1-1 Asahidai, Nomi, Ishikawa 923-1292, Japan*

(Dated: November 29, 2012)

Current computational capability allows a large-scale first-principles calculation, however, the heavily folded electronic band structure due to a big supercell suppresses an easy visualization of the effect of symmetry breakers introduced to the reference system. While an unfolding method has been proposed, a general formula is not yet available for a basis set of non-orthogonal atomic-like orbitals that is ideal for the unfolding concept due to the translational symmetric nature. In this study, we derive a simple formula applicable for both orthogonal and non-orthogonal localized orbitals. Codes using a basis set of linear combination of atomic-like orbitals, where the order-N method can be implemented much easier, can benefit from this approach in unfolding band structures. This method is applied for analysis of surface state with $ZrB_2(0001)$ surface and provides a way to examine how good a surface-sensitive measurement, like ARPES, can represent the bulk property. The effect of vacancies at various concentration levels in ZrB_2 will also be discussed.

PACS numbers: 71.15.-m,71.20.-b,79.60.-i

I. INTRODUCTION

The success of Kohn-Sham framework of density functional theory (DFT)[1] has led to extensive realization of solid state physics from the electronic band structures. One of the most utilized strategy to perform a first-principles calculation is the adoption of a supercell approach that makes studies of various forms of imperfections possible, for example, impurities, vacancies, a charge density wave, a spin density wave, and/or an orbital ordering introduced to extended systems.[2] Not restricted by the periodic boundary condition, the Bloch theorem can also be applied to study non-periodic systems, thank to the feasible computation of a big enough supercell that also allows one to investigate a system highly breaking the translational symmetry such as a presence of a surface.[3] However, a bigger supercell implies a smaller 1st Brillouin zone (BZ), as shown in Fig. 1, that highly suppresses an easy visualization of the effect of symmetry breakers introduced to the reference system due to the heavily folded bands in the 1st BZ that no longer resemble the original band structure anymore. A pioneering concept has been proposed to represent the spectral function, the imaginary part of retarded one-particle Green function, in the basis of the reference system, not the one of the supercell, allowing a direct comparison between first-principles calculations and angle resolved photoemission spectroscopy (ARPES).[4]

While the unfolding method has been introduced via the use of informative Wannier functions and gives rise to many detailed insights of physical understanding on various systems,[4–9] the construction of Wannier functions needs an additional effort from resulting Bloch states and might cost a non-negligible time for large-scale systems. Besides, the "unfolding" would physically make sense if the basis functions are almost identical between different reference unit cells, therefore, the Wannier function should be used with caution in unfolding the band structure, owing to the gauge freedom during the construction.[10] The unfolding method has also been introduced to the plane wave basis set, allowing an alternative option with different emphasis on physical properties.[11] In fact, both implementations imply an

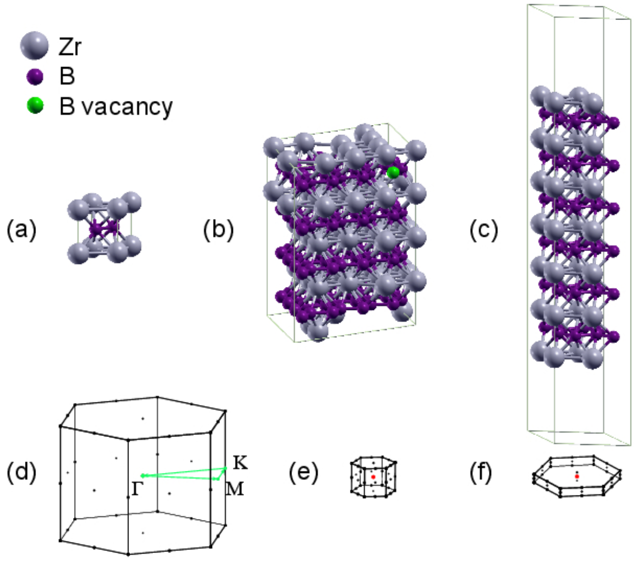

FIG. 1: Real-space unit cells of (a) normal-cell ZrB_2, (b) (4×4×4) supercell with a B vacancy, and (c) 13-layer slab. The corresponding 1st Brillouin zones are presented in (d), (e), and (f), respectively. Note that a nearly the same amount of states are accommodated in all illustrated zones, indicating a heavily folded feature of the supercell band structures.

orthonormal relationship for the smaller reference system. Given the translational symmetry has been broken in the actual supercell due to the presence of the symmetry breaker, it would be interesting to explore the unfolding method by using a translational symmetric basis, where the orthogonality nature must be broken.[12–17]

For studying a large-scale system, it is desirable to allow a linear scaling (order-N) computation that can highly optimize understanding of large-scale systems. It has been developed by using the basis of linear combination of atomic-like orbitals (LCAO).[13–19] Although the orthonormal relationship introduced for the unfolding method using Wannier functions cannot be directly applied for the LCAO basis without further orthonormalizing the basis functions, it provides another opportunity to explicitly take the overlap matrix of atomic-like orbitals, which are ideal for the unfolding concept, into account. In order to complement the current computational capability, it is timely to introduce a more general formula to optimize a deeper understanding of the effect of symmetry breakers in the band structures of large-scale systems with the LCAO basis.

II. OVERVIEW AND COMPUTATIONAL DETAIL

In this study, we derive a general formula in detail for unfolding electronic band structures applicable for both orthogonal and non-orthogonal basis sets via an introduction of the overlap matrix of localized orbitals. From that, it becomes clear on how an orthonormal basis set can simplify the calculation and on how good an approximation is if one chooses to neglect the non-orthogonality nature with a non-orthogonal basis set in order to reduce the computational time, which is illustrated with a study of (2×2×4) supercell without introducing any symmetry breaking. This method is applied for studying the proper spectral weight of $\mathrm{ZrB_2}$ with the presence of (1×1) and (2×2) unit cells of (0001) surface. The revealed spectral weight allows us to study if a surface component can represent the bulk band structure. Additionally, we have also investigated the effect of a low-concentration vacancy by introducing one Zr or one B vacancy in $\mathrm{Zr_{64}B_{128}}$ ($\mathrm{Zr_{0.984375}B_2}$ and $\mathrm{ZrB_{1.984375}}$) and have examined the applicability of a rigid band shift approximation upon doping for a metallic system.

The DFT calculations within a generalized gradient approximation[20] are performed by the OpenMX code,[12,21] which is based on norm-conserving pseudopotentials generated with multi reference energies and optimized pseudoatomic basis functions. The cut-off energy is set to 270 Ry and the basis functions of Zr$-s3p3d2$ and B$-s4p2d1$ are chosen with cut-off radius of 7 Bohr. The lattice constants of bulk $\mathrm{ZrB_2}$ converge to a=3.174Å and c=3.55Å with a 8×8×5 mesh of k points. The structure can be found in Fig. 1. The k points of supercell calculation are chosen to have the same quality of k mesh as the bulk one. The atomic positions are relaxed and the residual force on each atom is less than or equal to 3×10^{-4} Hartree/Bohr. The bulk lattice constants are in a good agreement with experimental data.[22]

III. DERIVATION OF PROPER SPECTRAL WEIGHT IN A NON-ORTHOGONAL BASIS

We now introduce a simple formula to unfold the band structure with the LCAO basis. The idea is to represent the spectral function in the LCAO basis of the reference system where a smaller normal unit cell is adopted. It is obvious that the unfolding process would reproduce the same result of the calculation of normal cell if the symmetry breaking is switched off in the supercell. Therefore, the strength of each band′s coupling to the symmetry breaker can be observed via the calculated spectral weight. One essential property of the LCAO basis is the non-orthogonality nature whose strength can be found from the overlap matrix elements of localized orbitals.[23] Since the overlap matrix elements and the LCAO coefficients of eigenstates at desired K points can be obtained from a regular band structure calculation of a big supercell, like the one provided by the OpenMX code, we assume those are available information and will derive a formula directly containing those two terms.

One can choose the K path to be outside the 1st BZ of the supercell to allow a comparison with the band structure along the k path in the normal-cell BZ. Although the K point outside the 1st BZ gives the same eigenstates (therefore, the same LCAO coefficients) as the one inside the 1st BZ connected by reciprocal lattice vectors (G) of the supercell (will be referred to $\delta_{k,[K]}$), the corresponding spectral weight is modified due to the new representation. The proper spectral weight, $A(\omega)$, represented by the conceptual normal-cell eigenstate $|kj\rangle$ (lowercase letters) can be obtained via this formula:

$$\begin{aligned}
&\sum_{kj}\langle kj|A(\omega)|kj\rangle \\
&= \sum_{kjmnm'n'} \langle kj|km\rangle S^{-1}_{mn}(k)\langle kn|A|km'\rangle S^{-1}_{m'n'}(k)\langle kn'|kj\rangle \\
&= \sum_{kmnm'n'} \langle kn'|km\rangle S^{-1}_{mn}(k)\langle kn|A|km'\rangle S^{-1}_{m'n'}(k) \\
&= \sum_{kmnm'n'} S^{-1}_{m'n'}(k) S_{n'm}(k) S^{-1}_{mn}(k)\langle kn|A|km'\rangle \\
&= \sum_{kmn} S^{-1}_{mn}(k)\langle kn|A|km\rangle .
\end{aligned} \tag{1}$$

The overlap matrix, $S(k)$, does not follow the orthonormal relationship in general and can not be neglected. By inserting known information, such as a supercell representation (uppercase letters) in real space ($\sum_{RMR'M'}|RM\rangle S^{-1}_{RM,R'M'}\langle R'M'|$) or the supercell eigenstate ($\sum_{KJ}|KJ\rangle\langle KJ|$) in this study, the spectral function at each k becomes:

$$\begin{aligned}
&\sum_j A_{kj,kj}(\omega)\\
&= \sum_{mnKJ} S^{-1}_{mn}(k)\langle kn|KJ\rangle\langle KJ|A|KJ\rangle\langle KJ|km\rangle\\
&= \sum_{mnKJMN} S^{-1}_{mn}(k)\langle kn|KN\rangle C^{KJ}_N\langle KM|km\rangle C^{KJ^*}_M A_{KJ,KJ}(\omega)
\end{aligned} \tag{2}$$

C^{KJ}_N denotes the LCAO coefficients of an eigenstate $|KJ\rangle$, such that $|KJ\rangle = \sum_N C^{KJ}_N|KN\rangle$.

Following the concept of unfolding, it is desirable to relabel the supercell orbital $|RN\rangle$ by the normal-cell $|rn\rangle$ and find the corresponding inner product:

$$\begin{aligned}
&\langle rn|RN\rangle\\
&= \langle rn|R + r_0(N), n'(N)\rangle\\
&= \sum_{k'}\langle rn|k'n\rangle\langle k'n|k'n'(N)\rangle\langle k'n'(N)|R + r_0(N), n'(N)\rangle\\
&= \sum_{k'}\frac{e^{ik'(r-R-r_0(N))}}{l}S_{nn'(N)}(k').
\end{aligned} \tag{3}$$

N labels the supercell orbital and $n(N)$ indicates which orbital the N belongs to in the normal cell. In order to employ Eqn. 3, we can insert real-space lattice vectors in Eqn. 2. Finally, the spectral function in the normal-cell representation can be derived in Eqn. 5 by directly containing LCAO coefficients and the overlap matrix of localized orbitals.

The spectral weight of an eigenstate of the supercell, $A_{KJ,KJ}(\omega)$, is just a delta function at the corresponding eigenvalue, therefore, one can calculate the spectral weight individually, for example, only the eigenstates within an energy window is needed in actual calculation. $L(l)$ denotes the number of $K(k)$ points in the supercell (normal-cell) first Brillouin zone and $\frac{L}{l}$ is the ratio of the volume of 1st BZ of the supercell to the normal-cell one. In the last step of derivation in Eqn. 5, the overlap matrix element $\langle R'M|r'n'(N)\rangle$ has been reduced to the one with $R' = 0$ for a periodic system:

$$\begin{aligned}
&\sum_{r'R'} e^{-iKR'}e^{ikr'}\langle R'M|r'n'(N)\rangle\\
&= \sum_{r'R'} e^{-i(k-G)R'}e^{ikr'}\langle R'M|r'n'(N)\rangle\\
&= \sum_{R'} e^{iGR'}\sum_{r'} e^{-ik(R'-r')}\langle R'M|r'n'(N)\rangle\\
&= \sum_{R'} e^{iGR'}\sum_{r'} e^{ikr'}\langle 0M|r'n'(N)\rangle\\
&= L\sum_{r'} e^{ikr'}\langle 0M|r'n'(N)\rangle.
\end{aligned} \tag{4}$$

$S(R = 0, M; r, n(N))$ denotes the overlap matrix elements including all non-zero contribution after a relabeling with the lattice vector r and the orbital n of the normal cell.

$$\begin{aligned}
\sum_j A_{kj,kj}(\omega) &= \sum_{mnKJMNrr'RR'} S^{-1}_{mn}(k)\langle kn|rn\rangle\langle rn|RN\rangle\langle RN|KN\rangle C^{KJ}_N\langle KM|R'M\rangle\langle R'M|r'm\rangle\langle r'm|km\rangle C^{KJ^*}_M A_{KJ,KJ}(\omega)\\
&= \sum_{mnKJMNrr'RR'} S^{-1}_{mn}(k)\frac{e^{-ikr}}{\sqrt{l}}\langle rn|RN\rangle\frac{e^{iKR}}{\sqrt{L}}C^{KJ}_N\frac{e^{-iKR'}}{\sqrt{L}}\langle R'M|r'm\rangle\frac{e^{ikr'}}{\sqrt{l}}C^{KJ^*}_M A_{KJ,KJ}(\omega)\\
&= \sum_{mnKJMNrr'RR'k'} S^{-1}_{mn}(k)\frac{e^{-ikr}}{\sqrt{l}}\frac{e^{ik'(r-R-r_0(N))}}{l}S_{nn'(N)}(k')\frac{e^{iKR}}{\sqrt{L}}C^{KJ}_N\frac{e^{-iKR'}}{\sqrt{L}}\langle R'M|r'm\rangle\frac{e^{ikr'}}{\sqrt{l}}C^{KJ^*}_M A_{KJ,KJ}(\omega)\\
&= \sum_{mnKJMNr'RR'} S^{-1}_{mn}(k)\frac{e^{-ik(R+r_0(N)-r')}}{lL}S_{nn'(N)}(k)e^{iK(R-R')}C^{KJ}_N\langle R'M|r'm\rangle C^{KJ^*}_M A_{KJ,KJ}(\omega)\\
&= \sum_{KJMNr'RR'} \frac{e^{-ik(R+r_0(N)-r')}}{lL}e^{iK(R-R')}C^{KJ}_N\langle R'M|r'n'(N)\rangle C^{KJ^*}_M A_{KJ,KJ}(\omega)\\
&= \sum_{KJMNr'R'} \frac{e^{-ik(r_0(N)-r')}}{l}e^{-iKR'}\delta_{k,[K]}C^{KJ}_N\langle R'M|r'n'(N)\rangle C^{KJ^*}_M A_{KJ,KJ}(\omega)\\
&=\frac{L}{l}\sum_{KJMNr'} e^{ik(r'-r_0(N))}\delta_{k,[K]}C^{KJ}_N\langle 0M|r'n'(N)\rangle C^{KJ^*}_M A_{KJ,KJ}(\omega)\\
&=\frac{L}{l}\sum_{KJMNr} e^{ik(r-r'(N))}\delta_{k,[K]}C^{KJ}_N S(0M, rn(N))C^{KJ^*}_M A_{KJ,KJ}(\omega).
\end{aligned} \tag{5}$$

Clearly, the effect of translational symmetry breaking has been not only recorded in the supercell eigenstates but also connected via the overlap matrix elements that are essential to deliver a complete spectral weight in the new representation. Note that this formula is in fact a more general formula for a basis set of localized orbitals and can be applied for both orthogonal and non-orthogonal orbitals by providing the corresponding S. It is obvious that the summation can be reduced by an adoption of orthogonal basis. Instead of carrying the relative phase from the distance between a lattice vector r and a $r'(N)$ weighted by the overlapping between $|0M\rangle$ and $|rn(N)\rangle$ orbitals to give rise to the corresponding contribution of $|KM\rangle$ and $|KN\rangle$, only the absolute r vector in a supercell is needed.

Since S decays rapidly due to the localized character of LCAO basis, it could be a good approximation to assume an orthonormal relationship, especially for occupied bands. However, it should be checked carefully in case of existence of strong effects from the non-orthogonality nature in studied cases. Nevertheless, the complete proper spectral weight in non-orthogonal basis only involves a simple summation with appropriate phases and directly uses the information from a regular band structure calculation, allowing an easy implementation. Finally, an arrangement of this formula by separating the summation of orbital index, e.g. $\sum_j A_{kj,kj}(\omega) = \sum_M W_M$, further provides the corresponding orbital contribution W_M in the unfolded band structure.

IV. ASSUMPTION OF ORTHONORMAL RELATIONSHIP IN LCAO BASIS

One can study how good an approximation is by assuming an orthonormal relationship even with the use of non-orthogonal LCAO basis. We illustrate an example of a (2×2×4) supercell calculation without introducing any symmetry breaking. Therefore, the unfolding process is expected to unfold the heavily folded band structure back to the normal-cell one exactly. We compare the unfolded band structures with and without the assumption of orthonormal relationship by tuning the overlap matrix S in Fig.2. As can be seen clearly, the unoccupied bands, where the eigenstates deviate from atomic orbitals much more, need large values of coefficients on non-orthogonal atomic orbitals and show strong disagreement. Without symmetry breaking, the deviation of occupied bands is small and the shadow bands show negligible intensity. Therefore, it could be a good approximation to assume the orthonormal relationship in unfolding occupied bands. This approximation is useful for a linear scaling calculation, where the one-particle Green function is usually obtained, not the LCAO coefficients, in estimating the unfolded band structure. Obviously, in order to deliver a complete spectral weight, one should not neglect the overlap matrix and one should check the approximation with caution, especially for the case with strong symmetry breaking.

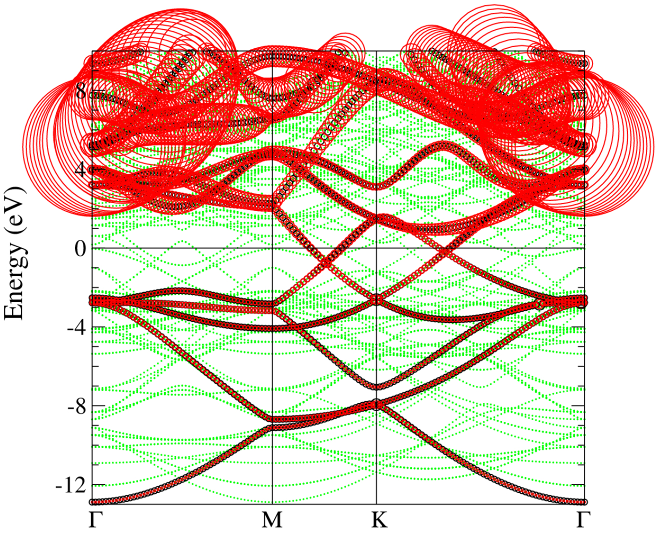

FIG. 2: Band structure of (2×2×4) supercell calculation of ZrB_2 without symmetry breaking. The result is presented in the first Brillouin zone of (1×1×1) normal cell. Unfolded band structures with and without the assumption of orthonormal relationship are presented by red and black circles, respectively, and the radius reflects the intensity of the proper spectral weight of each supercell eigenstate. The radius of red circle reflects how good the approximation is by comparing to the reference black circle. The degenerate eigenstates (energy difference less than 0.001 eV) are presented by one circle. The green dots show the band structure without unfolding from the (2×2×4) supercell calculation for comparison.

V. SURFACE STATE WITH ZIRCONIUM DIBORIDE (0001) SURFACE

A long standing issue on how good a surface-sensitive measurement, such as ARPES, can represent the bulk properties can be explicitly studied via unfolding. With the computational capability nowadays, the surface and bulk properties can be revealed via a slab calculation. Once the slab is thick enough, the middle part of the slab behaves as a bulk even with the presence of the surface. Therefore, the electronic band structure of such a slab exhibits both surface and bulk contributions simultaneously. Of course, a thicker slab is needed for a system with a strong interaction between surface and bulk layers. On the other hand, a bigger unit cell of studied surface is usually adopted in a common practice due to a spontaneous reconstruction[24] or an interaction with new added layers,[25,26] a simple projection of spectral weight on terminated layers can only reflect the spectral weight on the surface but cannot resolve the folding effect. The concept we have introduced is exactly aimed to unfold the band structure in relieving the complexity.

A graphene counterpart, silicene, has recently been epitaxially grown on the (2×2) unit cell of ZrB_2(0001) surface.[26] Without silicene, no surface reconstruction is found and only (1×1) unit cell is needed for studying ZrB_2(0001) surface.[27,28] Therefore, we use it as a case

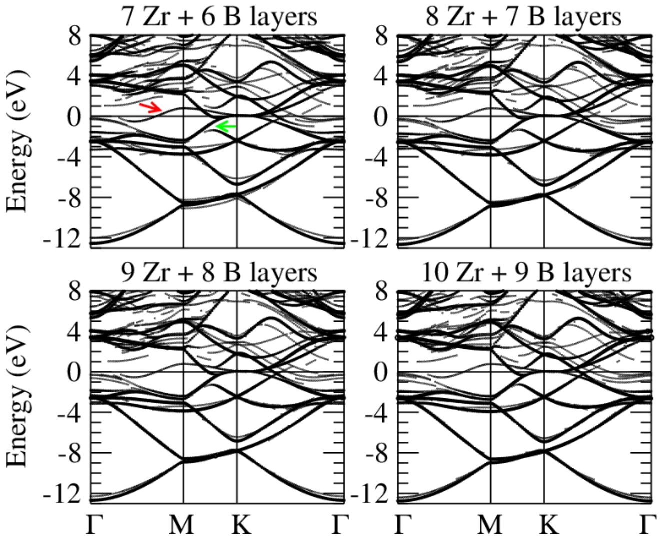

FIG. 3: Electronic band structures of Zr-terminated slabs for different layers with the presence of (2×2) unit cell of ZrB_2(0001) surface. The proper spectral weight of each supercell eigenstate in bulk representation is proportional to the radius of the corresponding circle. For a better visualization, the degenerate eigenstates (energy difference less than 0.001 eV) are presented by one circle. The dispersion curve indicated by the red arrow can be identified as the surface state and the gap opening deviating from the bulk band structure is pointed out by the green arrow.

study to investigate the proper spectral weight by performing a slab calculation with the (2×2) unit cell of ZrB_2(0001) surface and unfold the band structure to the (1×1×1) bulk representation. One can expect the unfolding method can recover the result of (1×1) unit cell of the surface from the introduced redundant (2×2) unit cell and can have an easy comparison with available results.[27,28]

After relaxing atomic positions in a slab with an additional empty layer (composed of LCAO basis of B atom with a flat zero potential) added into Zr terminated surface to have more complete information in the vacuum, band structures with different number of layers are presented in Fig. 3. Clearly, a band that cannot been identified in the normal-cell calculation [c.f. Fig. 5] crosses the Fermi energy between Γ and M in four different slab calculations and can be attributed as a surface state dispersion (red arrow). Note that the comparison of the band structure to the normal-cell one becomes easier in identifying the surface state due to unfolding the 1st BZ of (2×2) surface unit cell to the bulk one. Several shadow bands and gap opening can be observed due to the presence of the surface. Interestingly, while the surface state is converged with the number of layers and is good for a surface study, a gap opening between M and K at the Fermi energy (green arrow) is present even with the 19-layer slab calculation that deviates from the bulk band structure. One can see the gap closing converges slowly in Fig. 3, indicating a requirement of much more layers to capture the bulk band structure, highlighting the needs of a larger scale calculation and the unfolding method for it. It also reflects a deeper probe by a measurement is needed to observe a crossing dispersion between M and K below the Fermi energy.

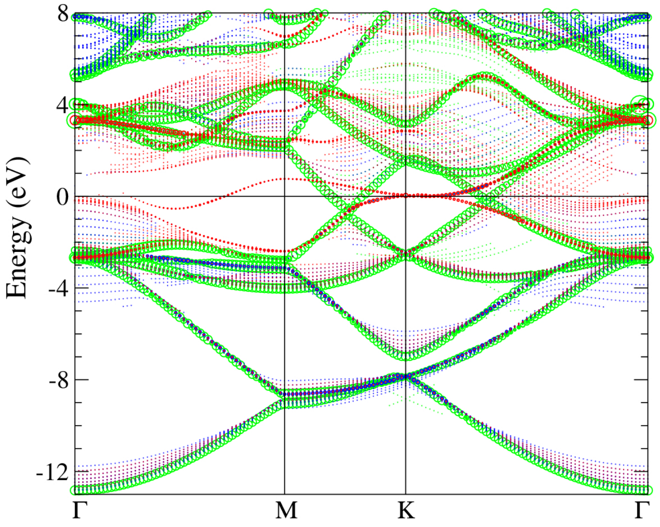

FIG. 4: Electronic band structure of Zr-terminated 59-layer slab with the presence of (1×1) unit cell of ZrB_2(0001) surface. The radii of circles are proportional to the positive contribution of proper spectral weight in the bulk representation. The red circles indicate the contribution of the two outermost Zr layers (four for two surfaces in a slab). The blue circles show the weight from the two outermost B layers (four for two surfaces in a slab). The rest contribution is presented by the green circle and reflects the bulk property. For a better visualization, the degenerate eigenstates (energy difference less than 0.001 eV) are presented by one circle and the radii of red and blue circles are doubled for comparison.

An advantage of the LCAO basis is the real-space representation that allows a useful analysis on the layer contribution of a slab in the band structure. In order to estimate the spectral weight of the surface, the positive contribution of W_M from the outermost layers is studied for a (1×1) unit cell of (0001) surface with 59 layers (30 Zr layers and 29 B layers). The one from two outermost Zr layers is shown in Fig. 4 by red circles. The outermost Zr layers not only contribute the spectral weight on the band of the surface state but also partly follow the normal-cell band structure. With unfolding, it is easy to see where the red circles deviate from the bulk bands (green circles) around the Fermi energy. Blue circles show the contribution from two outermost B layers. It is clear that the outermost ZrB_2 layers have already participated the bulk band structure by falling a weight on the contribution of rest layers (green circles). This advocates even a surface-sensitive measurement, like ARPES experiment, can access bulk band structures from several outermost layers. Of course, how deep the layer can reproduce the band structure of the middle part of a slab is case dependent and can be checked with a slab calcu-

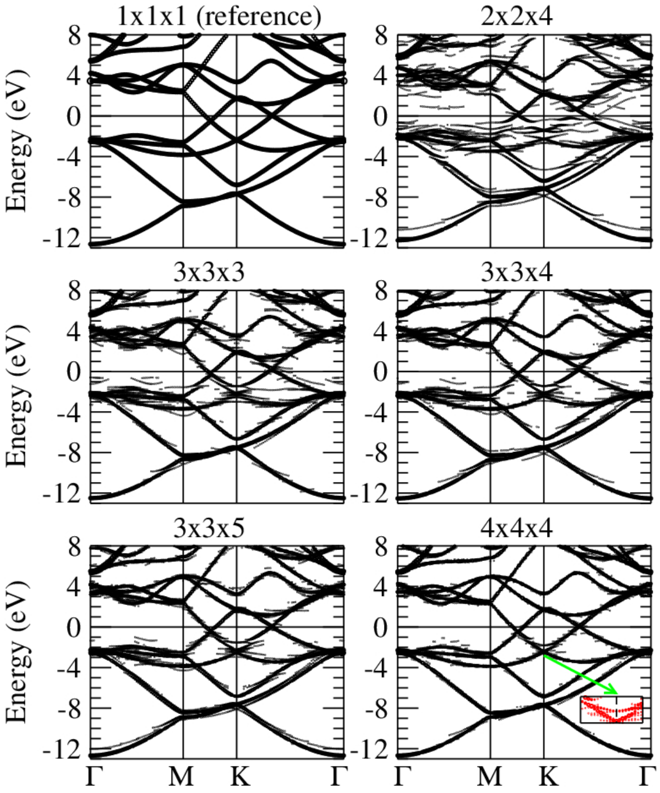

FIG. 5: Electronic band structures of a Zr vacancy introduced to the indicated supercells of ZrB_2. The (1×1×1) normal-cell band structure containing one Zr atom and two B atoms is presented as a reference for comparison. The proper spectral weight of each supercell eigenstate is proportional to the radius of the corresponding circle. For a better visualization, the degenerate eigenstates (energy difference less than 0.001 eV) are presented by one circle. For the (4×4×4) supercell case, although an overall spectral weight converges to the normal-cell one, gap openings still remain as indicated by the green arrow.

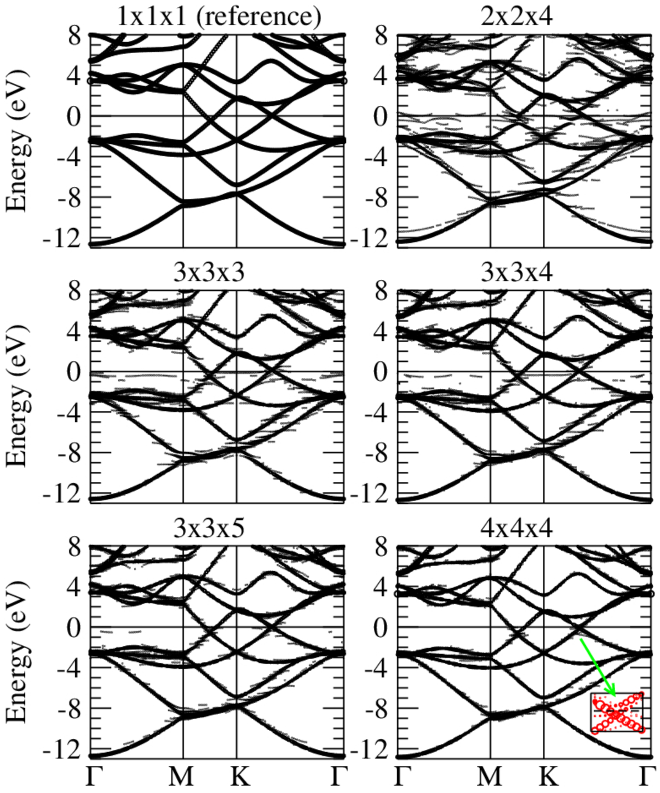

FIG. 6: Electronic band structures of a B vacancy introduced to the indicated supercells of ZrB_2. The (1×1×1) normal-cell band structure containing one Zr atom and two B atoms is presented as a reference for comparison. The proper spectral weight of each supercell eigenstate is proportional to the radius of the corresponding circle. For a better visualization, the degenerate eigenstates (energy difference less than 0.001 eV) are presented by one circle. For the (4×4×4) supercell case, although an overall spectral weight converges to the normal-cell one, a gap opening still remains as indicated by the green arrow.

lation in detail via unfolding.

VI. VACANCY STATE IN ZIRCONIUM DIBORIDE

A good approximation for studying the doping effect on the electronic band structure is the rigid band shift one that simply readjusts the Fermi energy of the normal-cell calculation according to the amount of electron or hole doping. This approximation makes sense if the introduced dopant interacts weakly with rest of the system. The applicability of this approximation can be visualized by comparing the calculations between a normal-cell band structure and a big supercell one via unfolding, not just a common comparison of density of states. One can expect as the supercell size becomes larger and lager, the normal-cell band structure can be recovered with a low-concentration disordered symmetry breaker, as can be observed by ARPES experiment, not the heavily folded bands fully occupying the supercell BZ. In Fig. 5 and 6, we show the band structures of ZrB_2 with one Zr and one B vacancy (replaced by an empty atom) [c.f. Fig. 1], respectively, in the indicated bigger supercells and compare to the (1×1×1) ZrB_2 whose 1st BZ is adopted to represent all results. As can be seen, the band structure becomes simpler and simpler with increased supercell sizes.

Not immune to the ordered vacancy we introduced to ZrB_2, especially the one in the smaller (2×2×4) supercell, prominent intensity of shadow bands and gap openings with considerable sizes can be observed, reflecting the strength of each band′s coupling to the translational symmetry breaker, which is the vacancy in this case. The band structures of (3×3×3) and (3×3×4) supercells show a tendency of convergence toward the normal-cell one. However, a flat band around the Fermi energy in Fig. 6 can be found that can significantly modify the conductivity for insulators due to the originally gapped band structure. For a metallic ZrB_2, the effect of vacancy states is not profound. Indeed, while the supercell size becomes larger, the normal-cell band structure can be recovered without prominent shadow bands and gap openings, advocating a rigid band shift approximation could be a good approximation if an overall band structure is concerned in the study of ZrB_2 with low-concentration vacancies. Nevertheless, one should realize the spectral weight does deviate from the normal-cell one more or less due to the vacancy even in the lowest concentration level we have studied, namely $\mathrm{ZrB}_{1.984375}$, and could perturb several physical properties, for example, a gap opening remains as indicated by the green arrow in Fig. 6 due to the ordered vacancy. Note that such gap opening can be observed easily from the unfolded band structure.

VII. SUMMARY

In summary, we offer a general formula to unfold first-principles band structures applicable for both orthogonal and non-orthogonal localized orbitals as basis functions. Codes using a LCAO basis set, which is suitable for a linear scaling calculation and for the unfolding concept, can directly implement such formula with a simple summation from a regular band structure calculation. Different from an orthogonal basis, the overlap matrix of localized orbitals plays an important role in connecting the recorded information of translational symmetry breaking in eigenstates. The LCAO basis contains real-space information that allows one can easily study the effect of symmetry breakers, such as the surface and the vacancy, in real space. By using ZrB_2 as a case study, we demonstrated unfolded band structures in the representation of the normal-cell 1st BZ with the presence of different concentration of vacancies and the surface. A slab calculation allows a straightforward way to compare with the band structure from a surface-sensitive measurement. By unfolding the band structure, the comparison with bulk states becomes easier in allowing identifying the surface state and the contribution of different layers can be further studied. In fact, several outermost layers are found to be able to exhibit most bulk band dispersion quite well. It is interesting to see if experiment can observe a crossing dispersion between M and K below the Fermi energy that belongs to the bulk property. Our method also shows a rigid-band shift approximation physically makes sense for a metallic ZrB_2 upon doping at low-concentration level. Benefiting from the unfolding method, a detailed study in the electronic band structure of a large-scale system is promising and the unfolded band structure can highly complement the information one can learn from density of states.

---

[1] W. Kohn and L. J. Sham, Phys. Rev. **140**, A1133 (1965).
[2] N. W. Ashcroft and N. D. Mermin, *Solid State Physics* (Holt, Rinehart, and Winston, New York, 1976).
[3] M. C. Payne, M. P. Teter, D. C. Allan, T. A. Arias, and J. D. Joannopoulos, Rev. Mod. Phys. **64**, 1045 (1992).
[4] W. Ku, T. Berlijn, and C.-C. Lee, Phys. Rev. Lett. **104**, 216401 (2010).
[5] C.-C. Lee, W.-G. Yin, and W. Ku, Phys. Rev. Lett. **103**, 267001 (2009).
[6] C.-H. Lin, T. Berlijn, L. Wang, C.-C. Lee, W.-G. Yin, and W. Ku, Phys. Rev. Lett. **104**, 216401 (2010).
[7] T. Berlijn, D. Volja, and W. Ku, Phys. Rev. Lett. **106**, 077005 (2011).
[8] S. Konbu, K. Nakamura, H. Ikeda, and R. Arita, J. Phys. Soc. Jpn. **80**, 123701 (2011).
[9] J.-S. Kang et al., Phys. Rev. B **85**, 085104 (2012).
[10] N. Marzari and D. Vanderbilt, Phys. Rev. B **56**, 12847 (1997).
[11] V. Popescu and A. Zunger, Phys. Rev. B **85**, 085201 (2012).
[12] T. Ozaki, Phys. Rev. B **67**, 155108 (2003).
[13] E. van Heumen et al., Phys. Rev. Lett. **106**, 027002 (2011).
[14] V. Blum et al., Comput. Phys. Commun. **180**, 2175 (2009).
[15] J. M. Soler et al., J. Phys. Condens. Matter **14**, 2745 (2002).
[16] M. J. Frisch et al., *Gaussian 09 Revision A.1*, gaussian Inc. Wallingford CT 2009.
[17] O. K. Andersen, Phys. Rev. B **12**, 3060 (1975).
[18] W. Yang, Phys. Rev. Lett. **66**, 1438 (1991).
[19] T. Ozaki, Phys. Rev. B **74**, 245101 (2006).
[20] J. P. Perdew, K. Burke, and M. Ernzerhof, Phys. Rev. Lett. **77**, 3865 (1996).
[21] T. Ozaki et al., URL `http://www.openmx-square.org/`.
[22] H. Li et al., Comput. Mater. Sci. **49**, 814 (2010).
[23] M. J. Han, T. Ozaki, and J. Yu, Phys. Rev. B **73**, 045110 (2006).
[24] M. Smeu et al., Phys. Rev. B **85**, 195315 (2012).
[25] C. Busse et al., Phys. Rev. Lett. **107**, 036101 (2011).
[26] A. Fleurence et al., Phys. Rev. Lett. **108**, 245501 (2012).
[27] T. Aizawa et al., Phys. Rev. B **71**, 165405 (2005).
[28] S. Kumashiro et al., e-J. Surf. Sci. Nanotech. **4**, 100 (2006).